

## MISTRAL@OHP OBSERVATIONS OF BOW-SHOCK STAR CANDIDATES

D. Russeil<sup>1</sup>, A. Zavagno<sup>1</sup>, J. C. Bouret<sup>1</sup>, C. Adami<sup>1</sup> and M. Dennefeld<sup>2</sup>

**Abstract.** Assuming that bow-shocks are produced by the interaction of the stellar winds with the interstellar medium we observed 47 bow-shock driving star candidates with the MISTRAL spectrograph at OHP. The goal is to confirm that OB stars are the main sources leading to the bow-shocks observed in the infrared.

Keywords: Stars, ISM:bow-shock

### 1 Introduction

Bow-shocks are arc-shaped structures located ahead a star and generally observed at mid-to-far IR wavelength. They are expected to result from the interaction of the stellar wind with the ambient interstellar medium (ISM). Two main categories can be distinguished: in-situ bow-shock and bow-shock due to a run-away star. When the star is a run-away it is its relative supersonic motion respectively to the ambient medium which creates the bow-shock. For in-situ bow-shock it is the flow of the local ISM in the direction of the star which creates it. In this poster we present a spectroscopic follow-up of a sample of 47 bow-shock driving star candidates in order to confirm the O or B spectral type of the driving star and to check, from GAIA DR3 astrometric data, their run-away status.

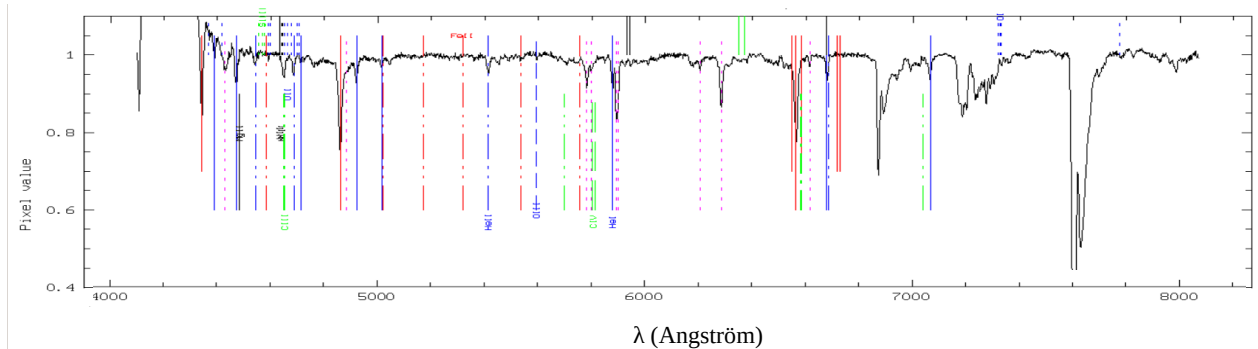


**Fig. 1.** Typical continuum normalised spectra observed with MISTRAL. The position of the lines (e.g. red, blue and blue dash-dot-dot labels for Hydrogen, HeI and HeII respectively) and diffuse interstellar bands (in magenta dashed) are identified.

The sample consists of 47 candidate bow-shock (BS) stars selected from the Jayasinghe et al. (2019) catalog and selected to be observable with the MISTRAL instrument ([http://www.obs-hp.fr/guide/mistral/MISTRAL\\_spectrograph\\_camera.shtml](http://www.obs-hp.fr/guide/mistral/MISTRAL_spectrograph_camera.shtml)) mounted at the T193 telescope to the Haute-Provence Observatory. The observations have been led with the blue objective. The spectral resolution is  $R = 709$  at  $6000\text{Å}$ . The data reduction has been led using the dedicated pipeline.

<sup>1</sup> Aix Marseille Univ., CNRS, CNES, LAM, 1388 Marseille, France

<sup>2</sup> Institut d'Astrophysique de Paris, 98bis Boulevard Arago, 75014 Paris, France

## 2 Spectral Classification

The spectral classification is commonly done from lines in the 4000-5000Å domain but, due to the low S/N ( $< 3$ ) we have in this spectral range we performed the spectral classification from lines in the red part (4500-7000Å) of the spectrum. Figure 1 shows a typical spectra with the main spectral features identified. We find that among the 47 candidates we have: 2 unclassifiable stars, 3 cool stars, 1 A-type star, 10 O stars and 31 B (mainly giants and super-giants) stars. **We confirm that bow-shocks are mainly driven by hot stars.**

## 3 Transverse Velocity

From the Gaia EDR3 (<https://www.cosmos.esa.int/web/gaia/early-data-release-3>) we retrieved the proper motions and the parallaxes for the sample stars which are used, following Russeil et al. (2020), to calculate the transverse velocity component of the stars in its local reference frame. We adopt the distance estimated from parallaxes by Bailer-Jones et al. (2021). If not available, the adopted distance is the spectrophotometric one. To ensure good quality, the transverse velocity ( $V_{\text{tan}}$ ) vector is calculated only for stars with  $\pi > 0$ ,  $\text{RUWE}^* \leq 1.4$ , and  $\sigma_{\pi} \leq 0.2$ . In this way, the transverse velocity could have been determined for 34 out of 47 sources. Figure 2 shows two examples of the transverse velocity vector respectively to the bow-shock. Regarding the angle ( $\alpha$ ) between the bow-shock axis and the  $V_{\text{tan}}$  direction the following results are obtained:

- 8 stars are well aligned and we note that they have the largest velocities (mean  $V_{\text{tan}} = 54.4 \text{ km s}^{-1}$ ) suggesting they are run-away.
- 15 stars have  $30^\circ \leq \alpha \leq 90^\circ$  (mean  $V_{\text{tan}} = 33.5 \text{ km s}^{-1}$ ).
- 11 move at the opposite direction (mean  $V_{\text{tan}} = 24.2 \text{ km s}^{-1}$ ), suggesting that in this case the bow-shock is an in-situ one.

**Our analysis indicates that bow-shocks are not only formed by run-away stars.**

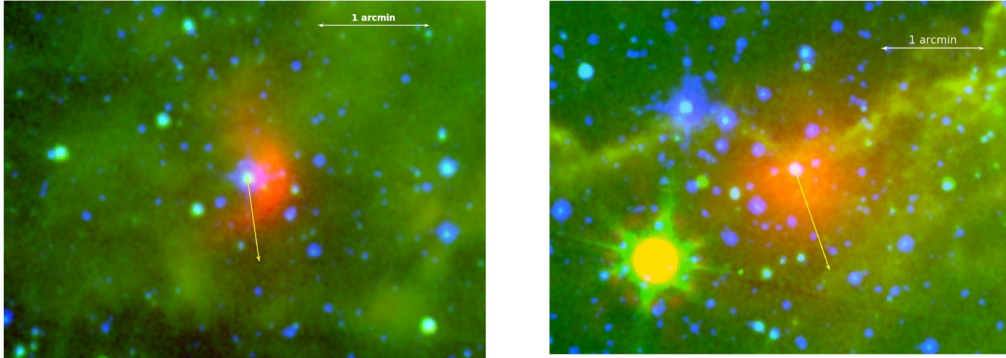


**Fig. 2.** Examples of the transverse velocity vector (yellow arrow, arbitrary scale) respectively to the bow-shock seen on the images as the red arc-shaped emission. The images combine the Spitzer-MIPS 24  $\mu\text{m}$  (red), Spitzer-IRAC 8  $\mu\text{m}$  (green) and DSS-RED (blue) images. The pictures show G0609757-0034412 (at 2 kpc) and G0629904-0043101 (at 4 kpc) respectively. With  $V_{\text{tan}} = 11.5 \text{ km/s}$  and  $V_{\text{tan}} = 55.3 \text{ km/s}$  respectively, only the second one is a run-away star.

## 4 Conclusion

Following these preliminary results we are dealing now with the ISM characterisation to clarify the context of each of these bow-shocks formation.

## References

- Bailer-Jones, C. A. L., Rybizki, J., Fouesneau, M., Demleitner, M., & Andrae, R. 2021, *AJ*, 161, 147  
 Jayasinghe, T., Dixon, D., Povich, M. S., et al. 2019, *MNRAS*, 488, 1141  
 Russeil, D., Zavagno, A., Nguyen, A., et al. 2020, *A&A*, 642, A21

\*The RUWE value is a measure of the reliability of the astrometric solution